

Electronic Structure and Thermoelectric Properties for Iodine Doped Clathrate Compounds

Takeshi Eto, Kenji Koga, Tatsuya Kamei, Koji Akai, and Mitsuru Matsuura

Faculty of Engineering, Yamaguchi University, Tokiwadai 2-16-1, Ube 755-8611, JAPAN

E-mail: matsuura@yamaguchi-u.ac.jp, Phone: +81-836-85-9620

Electronic structure of iodine doped type-I clathrate semiconductors is studied by the Full-potential Linearized Augmented Plane Wave method with the Generalized Gradient Approximation. The calculated band gaps of Sn_{46} , I_8Sn_{46} and $\text{I}_8\text{Sb}_8\text{Sn}_{38}$ are $E_g=0.68$ eV, 0.78 eV and 0.24 eV, respectively. Thus the I_8Sn_{46} has a wider band gap and I-doping causes the band gap widening. On the other hand, in $\text{I}_8\text{Sb}_8\text{Sn}_{38}$ anti-bonding Sb bands appear at the band gap and remarkable band gap narrowing occurs. The iodine p bands lie at valence bands and the density of states under the band gap becomes larger by I-doping. Especially the band structure with large density of states near the valence band edge appears in I_8Sn_{46} . The substitution of Sb broadens the large DOS peak due to the random potential effect of Sb ions. The Seebeck coefficient of $\text{I}_8\text{Sb}_8\text{Sn}_{38}$ has been calculated by using the calculated electronic structure. The result shows that the Seebeck coefficient is enhanced by the narrow iodine bands.

Key words: thermoelectric material, clathrate, FLAPW, Seebeck coefficient

1. INTRODUCTION

Recently, group-IV element (Si, Ge, Sn) clathrates have been attracting much attention as candidates of high performance thermoelectric materials and new type superconductors with complex crystal structures.[1, 2] The framework of group-IV element clathrates are composed of distorted tetrahedrons with sp^3 -like bonds. Though the coordination number and bonding nature is similar to that of cubic diamond materials, the morphology of crystal structures is much different. A lattice of the type-I clathrate consists of two kinds of nano-polyhedra: dodecahedra-cages and tetrakaidecahedra-cages that are linked by sharing faces, and a nano-cage network is fabricated. Alkali, alkaline earth or halogen atoms can be enclosed in cages and many kinds of elements can substitute for host atoms at the network sites. A varieties of controllable factors, i.e., doping elements, position of substitution and so on, influence various physical properties of the materials and therefore open up the possibility of hand-made material designs by the nano-structure operations.[3]

A concept of phonon glass and electron crystal (PGEC) is much concerned with high performance thermoelectric materials.[4] Clathrate semiconductors are the candidate for PGEC and much attention has been paid to Ba- and Na-doped clathrates. Concerned with halogen doping, an iodine doped clathrate $\text{I}_8\text{Si}_{44}\text{I}_2$ has been prepared by Reny *et al.* under the condition of high temperatures and high pressures, which is the first case of *p*-type silicon clathrate doped halogen.[5] In the $\text{I}_8\text{Si}_{44}\text{I}_2$, I atoms are perfectly positioned in nano-cages, and 11 % of Si 16i sites (*i.e.*, there are three distinct crystallographic sites; 6c, 16i and 24k in the framework of the type-I structure) is replaced with I atoms which are larger than the host Si atoms.[6] For the experimental studies of $\text{I}_8\text{Si}_{44}\text{I}_2$, Miguel *et al.* measured x-ray diffraction patterns under high pressures up to 35 GPa at room temperature, and estimated the pressure

dependence of the lattice parameter and the average first-neighbor Si-Si distances.[7] They found only the slight change in the lattice parameter at 17 GPa and confirmed more stable cage structure than $\text{Na}_8\text{Si}_{46}$ and $\text{Ba}_8\text{Si}_{46}$. Reny *et al.* measured the inelastic neutron scattering under ambient pressures at 300 K for A@Si_{46} (A: Na, K, Ba and I), and provided the spectra which is proportional to the phonon density of states.[8] By comparing the intensities of low-frequency modes corresponding to the vibrations of encaged atoms, they concluded that the coupling strength between guest atoms and host Si cages is the following order: $\text{Na} < \text{K} < \text{Ba} < \text{I}$. For the theoretical study of "ideal" I_8Si_{46} , Connetable *et al.* presented the first-principles calculations for the structural and electronic properties, and predicted that the strong hybridizations between the iodine and Si network orbitals result in a large opening of a 1.75 eV band gap.[9] Theoretical study of iodine doped Sn clathrates has not been calculated so far.

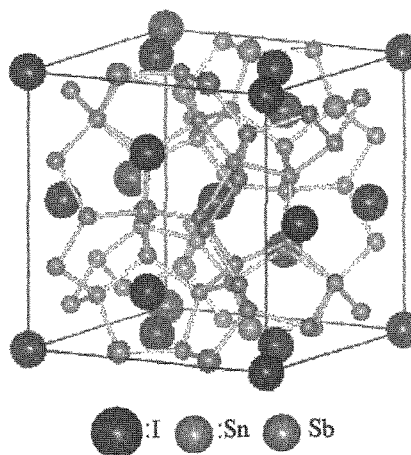


Fig. 1 Crystal structure of type-I $\text{I}_8\text{Sb}_8\text{Sn}_{46}$

Iodine doped Sn-base clathrate $I_8Sb_8Sn_{38}$ has been prepared by Muraoka *et al.* by using a mechanical alloying and Spark plasma sintering (SPS) method.[10] It shows high electric resistivity and *n*-type conduction.

Our purpose of this study is to calculate the electronic structures of iodine doped Sn clathrates using the *ab initio* method and to discuss an influence of iodine-doping on electronic transport properties from the point of view of the electronic structure.

2. COMPUTATIONAL DETAILS

The *ab initio* calculation is performed by using the full potential linearized augmented plane wave (FLAPW) method based on the density functional theory (DFT).[11] Figure 1 is a conventional unit cell of the type-I clathrate structure which has the simple cubic lattice and space group *Pm-3n* (No223). Iodine atoms occupy at $2a(0,0,0)$, $6d(0.25,0.5,0)$, and Sb or Sn atoms occupy at $6c(0.25,0,0.5)$, $16i(x,x,x)$ and $24k(0,y,z)$, respectively. In the present calculation, we used the following values for the APW parameters: $R_{mt}(I)=2.5a.u.$, $R_{mt}(Sb)=2.5a.u.$, $R_{mt}(Sn)=2.3a.u.$, $R_{mt} \cdot K_{max}=7$ and $G_{max}(a_0/2\pi)=14$. Here, R_{mt} is the muffin-tin radius, K_{max} is the plane-wave cutoff, G_{max} is the maximum magnitude of reciprocal lattice vectors which is used in the finite Fourier expansion of the electron density, and a_0 is a lattice constant. In the self-consistent calculation 36 k-sampling points are taken in an irreducible first Brillouin zone (BZ). For the exchange correlation potential we used the GGA of Perdew *et al.* [12]

Table I List of lattice parameters and bulk modulus of Sn_{46} , I_8Sn_{46} and $I_8Sb_8Sn_{38}$

	Sn_{46}	I_8Sn_{46}	$I_8Sb_8Sn_{38}$
a_0	12.377	12.328	12.326
(x, y, z)	(0.1831, 0.3099, 0.1161) ^a		
B_0 (GPa)	32.56	36.00	37.30
E_g (eV)	0.68	0.78	0.24

^aReference 5.

By using the linearized Boltzmann equation with the relaxation time approximation Seebeck coefficient α and the electric conductivity σ_e are given as

$$\alpha = \frac{8\pi e}{3T\sigma_e} \int d\varepsilon \left(-\frac{\partial f}{\partial \varepsilon} \right) \rho(\varepsilon) \tau(\varepsilon) v(\varepsilon)^2 (\varepsilon - \mu), \quad (1)$$

$$\sigma_e = \frac{8\pi e^2}{3} \int d\varepsilon \left(-\frac{\partial f}{\partial \varepsilon} \right) \rho(\varepsilon) \tau(\varepsilon) v(\varepsilon)^2, \quad (2)$$

where $\rho(\varepsilon)$, $\tau(\varepsilon)$ are the density of states, the relaxation time, μ is the chemical potential. In the present calculation the energy dependence of $\tau(\varepsilon)$ is neglected. Then the τ included in (1) and in σ_e cancel out each other and α becomes independent of τ . The velocity density $v(\varepsilon)$ is given as

$$v(\varepsilon)^2 \rho(\varepsilon) = \sum_{nk} \left| \frac{\partial \varepsilon_{nk}}{\hbar \partial k} \right|^2 \delta(\varepsilon - \varepsilon_{nk}), \quad (3)$$

3. RESULTS AND DISCUSSION

a) Crystal structure and lattice parameters

Table I is a list of lattice parameters and bulk modulus of Sn_{46} , I_8Sn_{46} and $I_8Sb_8Sn_{38}$. The positional parameters

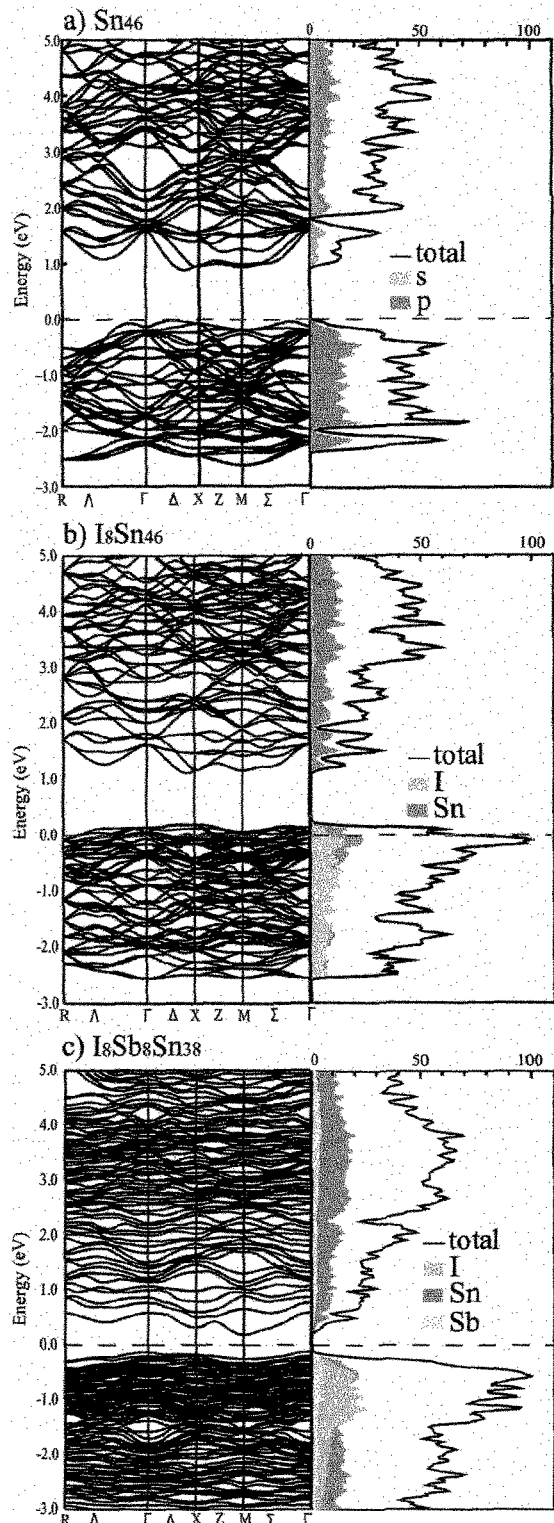


Fig. 2 Band structure and DOS. The energy is referred to the Fermi level

(x,y,z) were measured by Reny *et al.*[5] These lattice constants are obtained by the total energy calculation as a function of lattice constants. The calculated lattice constant of I_8Sn_{46} is 4 % smaller than of Sn_{46} and iodine doping shrinks the lattice constant. As the iodine ion is an anion and the Sn-cage has positive charge, the cage size become small by the ionic force. In the Si case the

lattice constant becomes large. It indicates that the Sn-cage is large enough for rattling in the cage and thereduction of lattice thermal conductivity is expected.

In Fig. 1 the Sb configuration is shown, which is used to calculate the electronic structure and the Seebeck coefficient of $I_8Sb_8Sn_{38}$. We calculate the total energy for several Sb-configuration cases: the Sb-Sb bonding case and the non Sb-Sb bonding case, and it is founded that the total energy of the non Sb-Sb bonding case is lower than of the Sb-Sb bonding case. Thus the Sb configuration shown in Fig. 1 has no Sb-Sb bonds.

b) Band structure

Band structure and density of states (DOS) of Sn_{46} , I_8Sn_{46} and $I_8Sb_8Sn_{38}$ are shown in Fig. 2. The unit of DOS is states/eV·cell. Broken lines denote the Fermi level, i.e., the top of valence bands.

Firstly, figures 2a and 2b show the I-doping effect on electronic structure. In Fig. 2a Sn type-I clathrate is an indirect-gap semiconductor with $E_g=0.68$ eV in which the k positions of the top of valence bands and of the bottom of conduction bands are slightly different, though both of the k positions are on the Δ -symmetry axis. This situation also holds in I_8Sn_{46} . The band structure of I_8Sn_{46} near the band gap is similar to that of

Sn_{46} and then the band gap is 0.78 eV. It is very different from the band structure on Si-base iodine clathrate because the conduction band structure of Si_{46} is drastically modified by iodine doping due to orbital hybridization between atomic states of I and of Si.[9] The lattice constant of I_8Sn_{46} is about 22 % larger than that of Si_{46} . The larger size of host cages may cause reduction of the hybridization. The band gap widening effect due to the iodine doping becomes also small, but the band gap is spread about 34 % compared with of Sn_{46} , and the iodine doping is much effective for band gap widening.

Secondly, I atoms in I_8Sn_{46} act as acceptors with an excess hole per atom and the Fermi level lies in valence bands. The Fermi level is 0.13 eV lower than the top of the valence band. It indicates that the I_8Sn_{46} behaves as heavily doped p -type semiconductor. In Fig. 2b large DOS states are seen under the Fermi level. The DOS is brought from p -states of Sn and I atoms. The DOS of valence bands are increased by iodine p -bands. The relative energy positions between p -orbital of I atoms and p -orbital of Sn atoms are modified by charge transfer from p -bands of Sn cages to p -orbital of I atoms. As seen in the DOS of Fig. 2b the shape of the partial DOS of I atoms resembles that of Sn atoms and it shows that p -orbital of I atoms hybridize with p -band of cage states strongly.

Thirdly, dopants Sb in $I_8Sb_8Sn_{38}$ act as donors and compensate for excess carriers. Thus, $I_8Sb_8Sn_{38}$ clathrate is an intrinsic semiconductor as seen in Fig. 2c and then the band gap is $E_g=0.24$ eV. The magnitude of the band gap is very different from of I_8Sn_{46} . The Sb doping causes strong band gap narrowing. The figure 3 shows the total and partial DOS of $I_8Sb_8Sn_{38}$. In the figure of partial DOS for each atom the orbital characters are shown. The shape of partial DOS of Sb is similar to that of Sn and thus it seems that Sb-Sn bonds are similar to Sn-Sn bonds and the carrier compensation by Sb doping works well from the point of view of the electron network. The partial DOS of I has a broad peak whose width is about 1 eV under the Fermi level, and the Sn and the Sb DOSs have also a small peak in the same energy region, respectively in Fig. 3. The effect of state hybridization between guest I atoms and host atoms on the DOS is similar to the case of I_8Sn_{46} , but the peak width is wider than in the case of I_8Sn_{46} . It is guessed that the DOS broadening is caused by the random potential effects due to Sb doping, i.e., Sb ions that are cations are randomly doped at Sn sites and therefore Madelung potential is different in atomic sites.

In the conduction band there is the pseudo-gap near 2 eV. The pseudo-gap appears in DOS of Sn_{46} and I_8Sn_{46} . The band below the pseudo-gap is dominantly composed of s orbital of host atoms and the band above that is of p orbital. The difference between the Sb doping case and the non-Sb doping case is the width of the lower bands: about 2 eV in $I_8Sb_8Sn_{38}$ and about 1 eV in I_8Sn_{46} and Sn_{46} . The anti-bonding Sb bands characterized by s band lie in the band gap and the band gap become narrow strongly.

c) Seebeck coefficient

The calculated Seebeck coefficient of p -doped $I_8Sb_8Sn_{38}$ is shown in Fig. 4 as a function of temperature

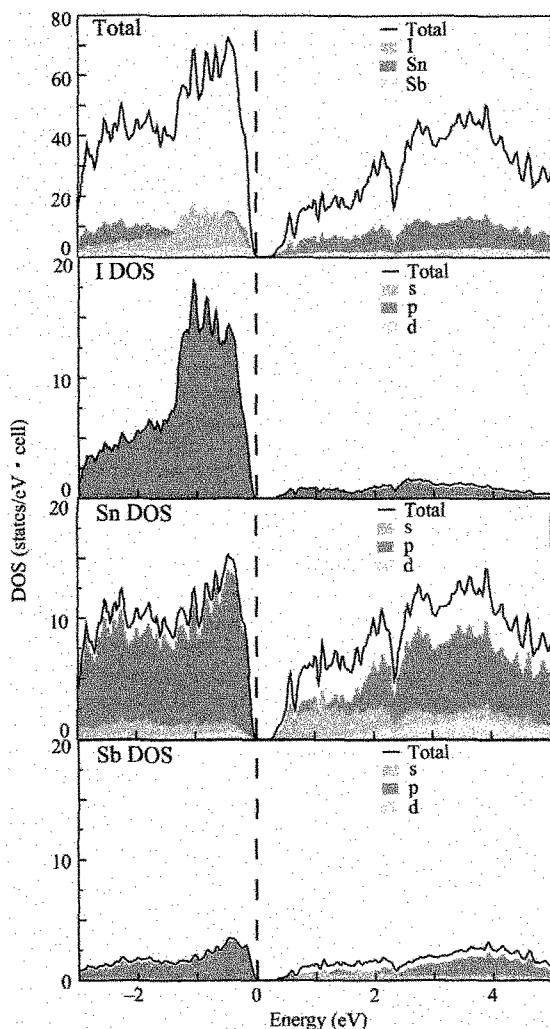


Fig. 3 Total and partial DOS for Sn, I and Sb in $I_8Sb_8Sn_{38}$

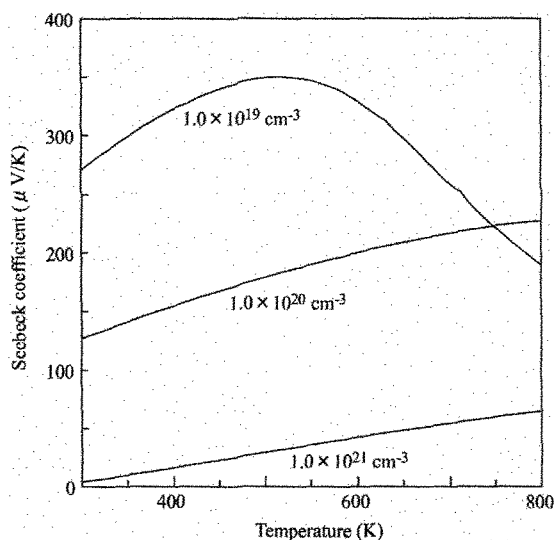


Fig. 4 The Seebeck coefficient of p-doped $I_8Sb_8Sn_{38}$ as a function of temperature.

by assuming the rigid band between room temperatures and 800 K. The Seebeck coefficient is calculated in three hole concentration cases: $1 \times 10^{19} \text{ cm}^{-3}$, $1 \times 10^{20} \text{ cm}^{-3}$ and $1 \times 10^{21} \text{ cm}^{-3}$. In the case of $1 \times 10^{19} \text{ cm}^{-3}$ the largest value of the Seebeck coefficient is approximately 350 $\mu\text{V/K}$ at 500 K. The large Seebeck coefficient is caused by the flat iodine band as shown in Fig. 2c. The magnitude is large compared with the previous results of *n*-type $Ba_8Ga_{16}Ge_{30}$ and it indicates that the iodine-filled Sn-based clathrates are candidates for the high performance thermoelectric materials, [13] but the magnitude of Seebeck coefficient decreases rapidly with increasing temperature above 500 K. The origin of the decrease in the higher temperature region above 500 K is cancellation of the Seebeck effects due to electrons and holes that are excited from the valence band to the conduction band thermally. With increasing the hole concentration, this effect gradually became small together with decreasing of absolute value of the Seebeck coefficient as shown in Fig. 4. Thus to obtain a larger thermoelectric power at the high temperatures, about 800 K or more, a wider band gap in $I_8Sb_8Sn_{38}$ is needed.

4. SUMMARY

We have calculated the electronic structure of the clathrate Sn_{46} , I_8Sn_{46} and $I_8Sb_8Sn_{38}$ by using the FLAPW method with GGA. In I_8Sn_{46} , I atoms act as acceptors with an excess hole and it becomes a heavily doped p-type semiconductor and the band gap is 0.78 eV. Thus iodine filling is effective to widen the band gap. In $I_8Sb_8Sn_{38}$ a doped Sb acts as a donor and excess holes are compensated. Thus, $I_8Sb_8Sn_{38}$ became an intrinsic semiconductor. The band gap is 0.24 eV and turns small by Sb doping. The Seebeck coefficient is calculated in several hole concentration cases by using the calculated band structure of $I_8Sb_8Sn_{38}$. At $1 \times 10^{19} \text{ cm}^{-3}$ the highest Seebeck coefficient value is about 350 $\mu\text{V/K}$ at 500 K. It indicates that iodine filled Sn base clathrates are candidates for the high performance p-type thermoelectric material. Especially the enhancement of the thermoelectric performance is expected by

overcoming the band gap narrowing due to Sb doping.

References

- [1] G. S. Nolas, G. A. Slack and S. B. Schujman, "Recent Trends in Thermoelectric Materials Research I", Edit. T. M. Tritt, Academic Press (2001).
- [2] H. Kawaji, H. Horie, S. Yamanaka and M. Ishikawa, Phys. Rev. Lett., **20** (1995), 1427.
- [3] W. Lek NG, M. A. Lourenco, R. M. G. William, S. Ledain, G. Shao and K. P. Homewood, Nature (London) **410** (2001), 192.
- [4] B. C. Sales, D. Mandrus, B. C. Chakoumakos, V. Keppens, and J. R. Thompson, Phys. Rev. **B56** (1997), 15081.
- [5] E. Reny, S. Yamanaka, C. Cros and M. Pouchard, Chem. Commun. **2000** (2000), 2505.
- [6] E. Reny, S. Yamanaka, C. Cros and M. Pouchard, J. Phys.: Condens. Matter **14** (2002), 11233.
- [7] A. San-Miguel, P. Melinon, D. Connetable, X. Blasé, F. Tournus, E. Reny, S. Yamanaka and J. P. Itie, Phys. Rev. **B65** (2002), 054109.
- [8] E. Reny *et al.*, Phys. Rev. **B66** (2002), 014532.
- [9] D. Connetable, V. Timoshevskii, E. Artacho, and X. Blasé, Phys. Rev. Lett. **87** (2001), 206405.
- [10] T. Muraoka, K. Kishimoto and T. Koyanagi, private communication
- [11] P. Blaha, K. Schwarz, G. Madsen, D. Kvasnica and J. Luitz, program package WIEN2k, Technical University of Vienna (2001).
- [12] J. P. Perdew, S. Burke and M. Ernzerhof, Phys. Rev. **B77** (1996), 3865.
- [13] T. Kamei, K. Koga, K. Akai, K. Oshiro, M. Matsuura, Trans. Mat. Res. Jpn, **29** (2004), 3651.

(Received January 15, 2006; Accepted March 30, 2006)